Magnetic island dynamics in magnetic reconnection in UTST experiments

Cite as: Phys. Plasmas **25**, 012126 (2018); https://doi.org/10.1063/1.5006092
Submitted: 22 September 2017 • Accepted: 11 January 2018 • Published Online: 31 January 2018

S. Kamio, M. Inomoto, K. Yamasaki, et al.

Magnetic island dynamics in magnetic reconnection in UTST experiments

S. Kamio,[1,a)] M. Inomoto,[2] K. Yamasaki,[3] T. Yamada,[4] C. Z. Cheng,[5] and Y. Ono[2]
[1]*National Institutes of Natural Science, National Institute for Fusion Science, Toki, Gifu 509-5292, Japan*
[2]*The University of Tokyo, Kashiwanoha, Kashiwa, Chiba 277-8561, Japan*
[3]*Kyushu University, Kasuga, Fukuoka 816-8580, Japan*
[4]*Kyushu University, Motooka, Fukuoka 819-0395, Japan*
[5]*National Cheng Kung University, Tainan 70101, Taiwan*

(Received 22 September 2017; accepted 11 January 2018; published online 31 January 2018)

The dynamics of the magnetic island formed inside the reconnection current layer was investigated under the strong guide field in the UTST spherical tokamak merging experiment. A pair of proximately located O- and X-points was generated at ∼5 cm away from the other X-point. The formed O- and X-points immediately started to move toward the downstream region inside the current layer, but the O-point had larger velocity and caught up the preceding X-point within 0.5 μs. The results from Doppler spectroscopy indicated that the ion flow velocity had the intermediate value between the O- and X-point velocities, suggesting that the ions flowed with approximately the same velocity with the magnetic island. *Published by AIP Publishing.*
https://doi.org/10.1063/1.5006092

I. INTRODUCTION

The dynamics of magnetic reconnection has been studied for many years by a variety of approaches such as theoretical studies, numerical studies, space observations, and laboratory experiments. In a previous study of magnetic reconnection based on the magnetohydrodynamic (MHD) theory,[1] the evaluated reconnection time scale did not match the observations of the explosive reconnection events in space. Recent numerical and theoretical studies based on the "plasmoid induced" reconnection model in which magnetic islands are generated inside the current layer have shown large enhancement of the reconnection rate in a collisionless regime.[2–6] The magnetic reconnection process associated with island formation in the anti-parallel magnetic configuration has been also studied in laboratory experiments[7,8] and in spacecraft observations.[9] In these studies, magnetic islands were generated in a long elongated current layer due to the tearing instability.

Figure 1 shows the schematic view of high guide field magnetic reconnection with an island inside the current sheet. A guide field, which is the magnetic field component perpendicular to the reconnection magnetic field, exists in many reconnection cases. It is predicted that the guide field essentially changes the reconnection behavior, e.g., suppression of Hall effects,[10] asymmetric flow patterns,[11] and modified potential structures.[12] Magnetic reconnection in the presence of an extremely strong guide field is difficult to be conducted in numerical simulations because it requires small step size and small spatial mesh size due to the high electron cyclotron frequency and the small electron gyroradius. On the other hand, strong guide field reconnection takes place during the merging compression start-up of a spherical tokamak (ST) plasma as an efficient fusion core plasma. Recent results from the world largest ST experiment in the MAST device showed peaked electron temperature at the reconnection X-point.[13] The maximum electron temperature had a strong dependency on the strength of the guide field, but no detailed measurement of the magnetic field has been performed yet because of the experimental constraint. The laboratory experimental device UTST[14] also develops the merging compression start-up of ST plasma through magnetic reconnection in the presence of a guide field about 10–20 times as large as the reconnection field. The UTST experiment has large flexibility to conduct a reconnection experiment in the presence of a strong guide field. Different from the other reconnection experiments, the reconnection inflow is strongly driven by the motion of upstream plasmas approaching each other. In the UTST guide field reconnection experiments, soft X-ray emission[15] and line spectral emission from ions with high upper state energy,[16] e.g., He II and C III, were observed to localize in the vicinity of the reconnection point. These experimental results suggest that there should be a local electron heating/acceleration mechanism. Some particle simulation studies reported electron parallel acceleration in guide field reconnection.[17] In these simulations, however, the electrons quickly escaped from the current layer and accumulated in the downstream region. On the other hand, the UTST previous experiments showed that these emissions were observed only near the reconnection

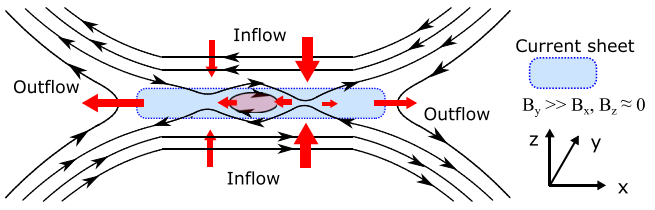

FIG. 1. Schematic view of high guide field magnetic reconnection with an island inside the current sheet indicated by the blue hatched region, where the in-plane magnetic field is much smaller that the out-of-plane (guide) magnetic field. Red arrows show the directions of the inflow and the outflow.

[a)]Electronic mail: kamio@nifs.ac.jp

point, suggesting some confinement mechanism of accelerated energetic electrons. One candidate as a confinement mechanism is the modification of the magnetic structure of the magnetic reconnection with an island structure which may confine the accelerated electrons inside the current sheet. In this paper, we will report the detailed dynamics of islands in magnetic reconnection with a strong guide field, using the magnetic probes, imaging camera, and spectroscopy.

II. EXPERIMENTAL SETUP

Figure 2 shows the cross-sectional view of the UTST device together with the experimental results from the magnetic measurement and fast camera imaging. Two initial STs are generated in upper and lower regions in the UTST vacuum chamber and merged at the center of the device ($z = 0$) through magnetic reconnection. Each of the two initial STs has both poloidal and toroidal comportments of the magnetic field. The poloidal fields in the two initial STs form an antiparallel structure of radial magnetic field B_r, that is, the reconnecting comportment. On the other hand, the toroidal fields in both STs are in the same direction, serving as a guide field perpendicular to the reconnection field. The inflow comes from upper and lower regions, and the outflow streams out to the radially inboard and outboard regions. Since the experiment has toroidal symmetry, the X-point forms a ring-shape along the toroidal direction, as indicated in Fig. 2. The ring-shaped structure was observed as a localized spectral line emission from carbon ions (C III 464.7 nm) by using a fast imaging camera with a band pass filter, as shown in the left side of Fig. 2.

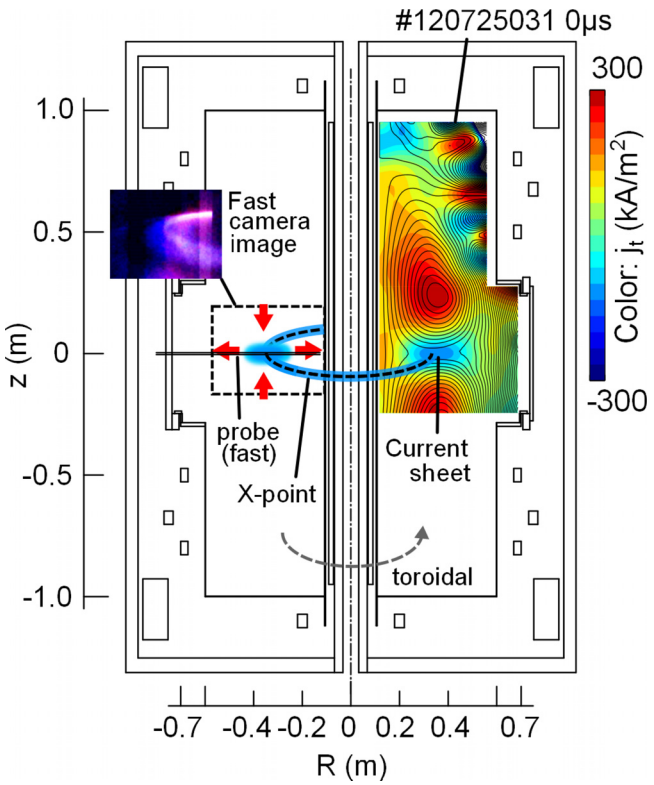

FIG. 2. The cross-sectional view of the UTST device. The contour plot in the right hand side of the UTST shows the experimentally observed magnetic flux together with the toroidal (out-of-plane) plasma current. The reconnection region was also observed by a fast imaging camera during the magnetic reconnection. The ring-shape emission region was observed along the current sheet as shown in the left side of the device. The magnetic probe for a high frequency signal is located at $z = 0$ m as shown in the left side. Red arrows show the directions of the reconnection inflow and the outflow.

The global magnetic field structure is observed by a two dimensional array of pick-up coils with windings of 300-turn to measure the axial magnetic field B_z and the toroidal (guide) magnetic field B_t at 145 locations with a radial spacing of 7 cm and an axial spacing of 6 cm. A typical magnetic field of the initial plasmas is ~250 mT in the toroidal direction and ~15 mT in the poloidal direction. This pick-up coil array provides a macroscopic field profile during reconnection; however, its spatial and temporal resolutions are not enough to detect the local behavior inside the current layer, whose typical thickness is shorter than 5 cm. Thus, we newly equipped a linear array of 22 high-frequency pick-up coils. Each coil has 15-turn windings with $\phi = 1.6$ mm, which is available up to 10 MHz. The coils measure the reconnected field B_z and are aligned in the radial direction with a spacing of 1 cm located at the center of the current layer $z = 0$ to resolve the finer and faster behavior of the reconnected magnetic field along the outflow direction. Since this high-frequency coil has lower sensitivity for low frequency signals, we combined the results from 15-turn (>33 kHz) and 300-turn (<33 kHz) coils to reconstruct the radial profile of reconnected magnetic field B_z with a wide frequency range of 1 kHz–10 MHz.

A multi-channel Doppler spectroscopy system was developed to measure the ion temperature and flow velocity. This system has eight wavelength channels in each of the spatial lines-of-sight with a time resolution of shorter than 1 μs.[18] In this experiment, we utilized the radial line-of-sight to measure the radial ion flow velocity. The plasma emission structure during magnetic reconnection shown in Fig. 2 was taken by a fast camera with a band pass interference filter with a center wavelength of 465 nm, which transmits the C III emission line of 464.7 nm. The C III emission region had a clear ring-like shape resembling the shape of the X-point possibly because the low state carbon ions are ionized and excited by energetic electrons which are accelerated in the toroidal direction by the reconnection electric field. Note that the excitation energy for the upper state of C III line emission is 32 eV, which is higher than the typical electron temperature of $T_e \sim 10$ eV measured by Thomson scattering. In the spectroscopy measurement, the He II 468 nm line is used to observe the bulk ion behavior near the X-point. The plasma is formed from helium gas, and we confirmed that the He II emission is also localized near the X-point region.[16]

Other typical parameters of helium plasma in the UTST experiments are the electron density $n_e \sim 10^{19}$ m^{-3} and the ion temperature $T_i \sim 10$–50 eV. The Alfven velocity is V_A ~50 km/s calculated by using the reconnecting component of the magnetic field. The magnetic Reynolds number of R_m ~10^2–10^3 for the helium discharge in UTST indicates that the collisionless condition is not satisfied. Thus, it is considered that the tearing instability that produces closed flux surfaces, the so-called "plasmoids," inside the current layer will not develop in the present experiment.

III. RESULTS AND DISCUSSIONS

Figure 3(a) shows the time evolution of the reconnection (toroidal) electric field at the X-point. Here, $t = 0$ represents the onset timing of magnetic reconnection. The reconnection electric field accelerates the electrons to generate the current sheet between the two approaching STs. The reconnection electric field in the range of 50–100 V/m was induced during the merging period of about 30–40 μs. Figure 3(b) shows the time evolution of the reconnected magnetic field B_z measured at 22 radial locations on $z = 0$. B_z was close to zero inside the current layer and had a positive value in the inboard side downstream region and a negative value in the outboard side downstream region. The black line indicates the B_z zero-crossing location, i.e., the poloidal (in-plane) field null point, of the magnetic reconnection. The magnetic structure inside the current layer showed dynamic behavior in terms of time and space particularly at $t > 6$ μs. The null (X) point repeated radially traveling motion inside the current layer. Note that multi-null points existed at several time points, suggesting the formation of an island with a closed flux surface. Figure 4 shows radial B_z profiles at four distinctive timings in Fig. 3(b). B_z crosses zero at three radial positions around $t = 7.2$ μs. The central null point corresponds to the island O-point accompanied by the X-point on each side. The whole island structure moved toward the inboard side, while the O-point moved faster than the X-point. The magnetic field inside the closed flux surfaces finally made a secondary reconnection with the downstream magnetic field. This series of motion corresponds to a streak-like structure which tracks the lower right direction in Fig. 3(b). After the

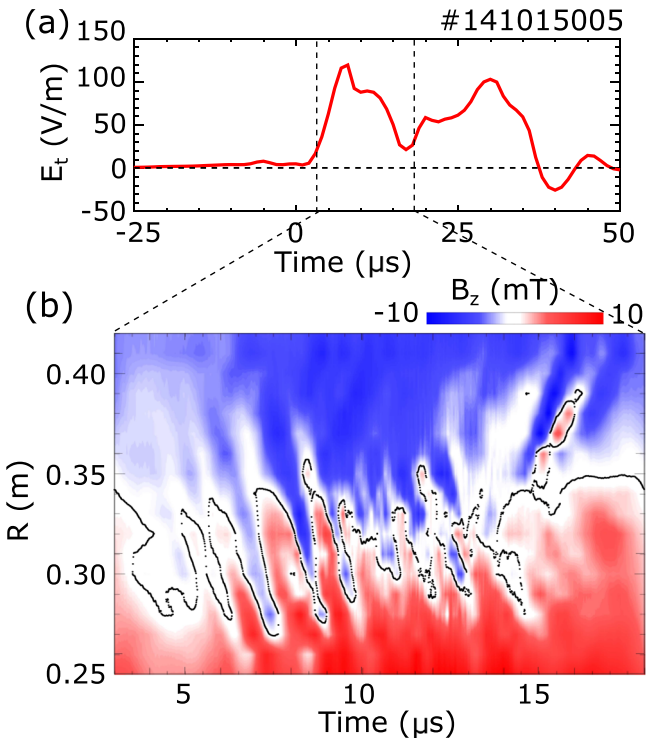

FIG. 3. (a) Time evolution of reconnection electric field E_t. (b) Time evolution of reconnected magnetic field B_z during the magnetic reconnection at $z = 0$ m, measured by the combination of two kinds of pick-up coils. The black line shows the position of the null point where $B_z = 0$ mT.

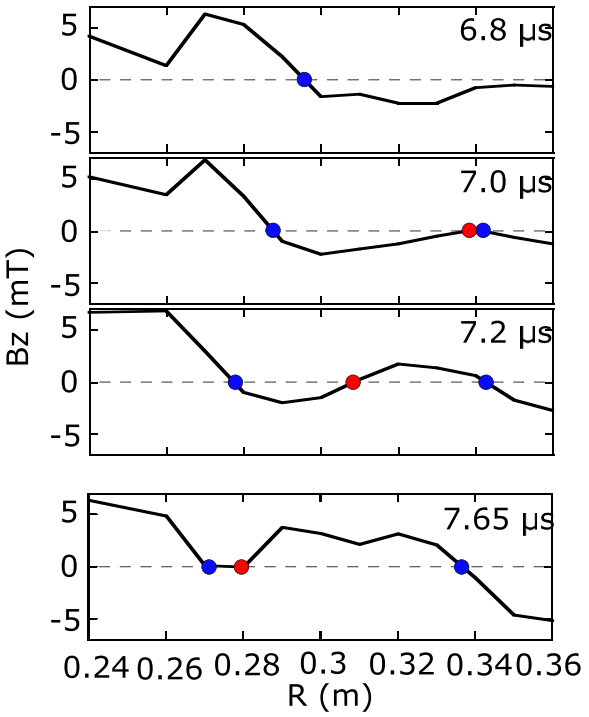

FIG. 4. Radial profiles of the reconnected magnetic field at $t = 6.8$, 7.0, 7.2, and 7.65 μs. The red circles indicate the O-points, and the blue circles indicate the X-points.

O-point disappeared, another pair of the O-point and the X-point was formed. The new O-point moved towards the inboard side for 5–6 times, but some O-points moved towards the outboard side in the later phase of $t > 13$ μs, as shown in Fig. 3(b).

The time evolution of radial positions and velocities of the null points is shown in Fig. 5. The red and blue curves indicate the motions of the O-point and the X-point, respectively. Three islands were formed in sequence at $R \sim 32$ m within 3 μs. The formed islands moved toward the inboard side, but the velocities of the X- and O-points did not match. Figure 5(b) shows the close-up of the velocity evolution from 6.5 to 8 μs. During this period, the averaged velocity of the X-points was about 20 km/s, but the O-points moved with a higher averaged velocity of about 80 km/s than the X-points. They caught up the inboard-side X-point within 0.5 μs after formation and annihilated through a secondary reconnection.

Figure 6 shows the time evolutions of the radial ion velocities measured by Doppler spectroscopy using He II line emission from two different discharges. Since the He II emission was localized around the current sheet region and the C III emission observed by the fast camera, the measured ion velocity is considered to represent the local ion flow velocity inside the current sheet. The ions were stationary at the beginning phase of the reconnection ($t < 5$ μs), and then, the radial velocity of up to ~40 km/s was observed. The direction of the ion motion changed from discharge to discharge or changed even in a discharge within several microseconds. The maximum ion flow velocity was lower than the velocity of the O-point but similar to the velocity of the X-points. The observed ion velocity is considered to reflect

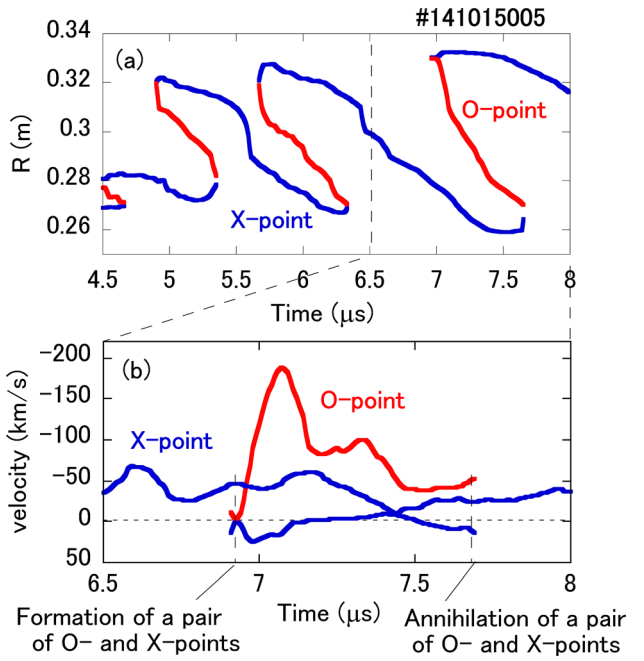

FIG. 5. (a) Time evolution of the positions of the O-points (red lines) and the X-points (blue lines) from 4.5 to 8 μs. (b) Time evolution of the velocities of the O-point (red line) and the X-points (blue lines) from 6.5 to 8 μs.

the averaged ion flow velocity inside the current layer. The observed ion flow was generally unidirectional when the generated islands traveled in one (inboard or outboard) direction. These results suggest that the ions inside the current layer travel in company with the island-like magnetic structure, which is considered to be formed by the localized electron current, at nearly the same velocity.

Figure 7 shows the illustration of the magnetic field structure at five distinctive timings based on the experimental results shown in Figs. 3–5. The radial positions of the X- and O-points in Fig. 7 match with the experimental results shown in Fig. 5(a). The internal structure inside the current layer has a comparable scale length as long as the length of the current layer. A sequence of the formation, radial translation, and annihilation of an island takes place in succession, and both the ions and electrons are transferred inside the current layer nearly at the same speed.

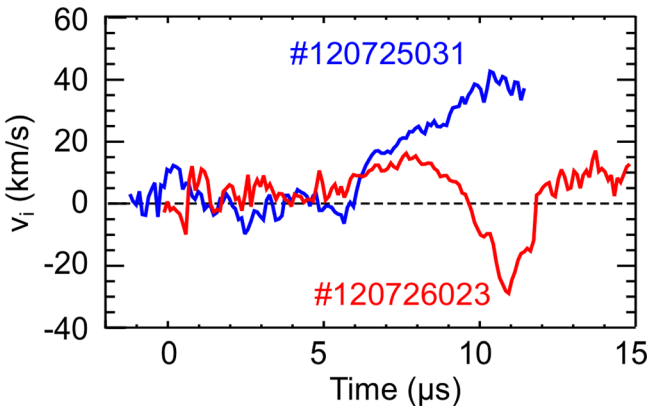

FIG. 6. Time evolution of the radial ion flow velocity observed by Doppler spectroscopy using line emission from helium ions in two discharges.

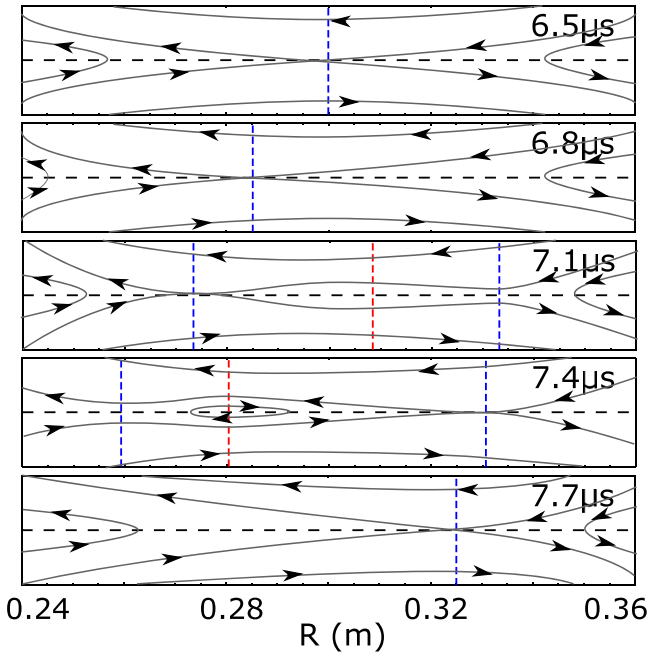

FIG. 7. Illustration of the magnetic field structure at five distinctive timings based on the experimental results shown in Figs. 3–5.

IV. SUMMARY

Repeated generation of magnetic islands with closed flux surfaces was observed in the magnetic reconnection current layer in the presence of a strong guide field in the UTST ST merging experiment. These islands moved toward the downstream region, but the velocity of the O- and X-points was different. The islands were transferred in association with the deformation of their shapes and finally collided with the downstream magnetic field and absorbed through secondary reconnection. These formation, radial motion, and secondary reconnection processes took place in every 1 μs and continued for $\sim$10 μs during the merging formation of ST plasma.

Since the observed current layer did not have an elongated shape, the tearing instability is not considered to be the origin of the islands because of the rather collisional experimental condition. The formation mechanism of the islands in this experiment is not clear at this moment but will be presented somewhere.

ACKNOWLEDGMENTS

This work was supported by the Grant-in Aid for Scientific Research (KAKENHI) Nos. 16K14525, 15H05750, 15K14279, and 26287143 and the NIFS Collaboration Research Program NIFS15KBAR012.

[1]E. N. Parker, J. Geophys. Res. **13**, 303 (1975).
[2]G. S. Choe and C. Z. Cheng, Astrophys. J. **541**, 449–467 (2000).
[3]C. Z. Cheng, Y. Ren, G. S. Choe, and Y.-J. Moon, Astrophys. J. **596**, 1341–1346 (2003).
[4]A. Bhattacharjee, Y.-M. Huang, H. Yang, and B. Rogers, Phys. Plasmas **16**, 112102 (2009).
[5]N. F. Loureiro, R. Samtaney, A. A. Schekochihin, and D. A. Uzdensky, Phys. Plasmas **19**, 042303 (2012).
[6]L. Comisso, M. Lingam, Y.-M. Huang, and A. Bhattacharjee, Phys. Plasmas **23**, 100702 (2016).

[7]J. Olson, J. Egedal, S. Greess, R. Myers, M. Cleark, D. Endrizzi, K. Flanagan, J. Milhone, E. Peterson, J. Wallace, D. Weisberg, and C. B. Forest, Phys. Rev. Lett. **116**, 255001 (2016).
[8]J. J. Almonte, H. Ji, M. Yamada, J. Yoo, and W. Fox, Phys. Rev. Lett. **117**, 095001 (2016).
[9]M. Oieroset, T. D. Phan, C. Haggerty, M. A. Shay, J. P. Eastwood, D. J. Gershman, J. F. Drake, M. Fujimoto, R. E. Ergun, F. S. Mozer, M. Oka, R. B. Torbert, J. L. Burch, S. Wang, L. J. Chen, M. Swisdak, C. Pollock, J. C. Dorelli, S. A. Fuselier, B. Lavraud, B. L. Giles, T. E. Moore, Y. Saito, L. A. Avanov, W. Paterson, R. J. Strangeway, C. T. Russell, Y. Khotyaintsev, P. A. Lindqvist, and K. Malakit, Geophys. Res. Lett. **43**, 5536–5544, https://doi.org/10.1002/2016GL069166 (2016).
[10]T. D. Tharp, M. Yamada, H. Ji, E. Lawrence, S. Dorfman, C. Myers, J. Yoo, Y. M. Huang, and A. Bhattacharjee, Phys. Plasmas **20**, 055705 (2013).
[11]M. Hesse, N. Aunai, S. Zenitani, M. Kuznetsova, and J. Birn, Phys. Plasmas **20**, 061210 (2013).
[12]W. Fox, F. Sciortino, A. V. Stechow, J. Jara-Almonte, J. Yoo, H. Ji, and M. Yamada, Phys. Rev. Lett. **118**, 125002 (2017).
[13]T. Yamada, H. Tanabe, T. G. Watanabe, Y. Hayashi, R. Imazawa, M. Inomoto, Y. Ono, M. Gryaznevich, R. Scannell, C. Michael, and The MAST Team. Nucl. Fusion **56**, 106019 (2016).
[14]M. Inomoto, T. G. Watanabe, K. Gi, K. Yamasaki, S. Kamio, R. Imazawa, T. Yamada, X. Guo, T. Ushiki, H. Ishikawa, H. Nakamata, N. Kawakami, T. Sugawara, K. Matsuyama, K. Noma, A. Kuwahata, and H. Tanabe, Nucl. Fusion **55**, 033013 (2015).
[15]T. Ushiki, M. Inomoto, K. Yamasaki, X. Guo, T. Sugawara, K. Matsuyama, H. Kocuchi, and T. Yamada, Plasma Fusion Res. **11**, 2402100 (2016).
[16]S. Kamio, K. Yamasaki, K. Takemura, Q. H. Cao, T. G. Watanabe, H. Itagaki, T. Tsutsui, K. Ishiguchi, R. Imazawa, T. Yamada, C. Z. Cheng, M. Inomoto, Y. Takase, and Y. Ono, IEEJ Trans. Fundam. Mater. **133**, 166 (2013).
[17]J. F. Drake, M. Swisdak, H. Che, and M. A. Shay, Nature **443**, 553 (2006).
[18]S. Kamio, N. Suzuki, Q. H. Cao, T. G. Watanabe, K. Abe, M. Sakumura, K. Ishiguchi, R. Imazawa, T. Yamada, M. Inomoto, Y. Takase, and Y. Ono, Rev. Sci. Instrum. **83**, 083103 (2012).